Laser emissions from one-dimensional photonic crystal rings on silicon-dioxide

Tsan-Wen Lu, Wei-Chi Tsai, Tze-Yao Wu, and Po-Tsung Lee

Citation: Applied Physics Letters **102**, 051103 (2013); doi: 10.1063/1.4790618
View online: http://dx.doi.org/10.1063/1.4790618
View Table of Contents: http://scitation.aip.org/content/aip/journal/apl/102/5?ver=pdfcov
Published by the AIP Publishing

APPLIED PHYSICS LETTERS **102**, 051103 (2013)

Laser emissions from one-dimensional photonic crystal rings on silicon-dioxide

Tsan-Wen Lu, Wei-Chi Tsai, Tze-Yao Wu, and Po-Tsung Lee[a)]
Department of Photonics and Institute of Electro-Optical Engineering, National Chiao Tung University, Rm. 413 CPT Building, 1001 Ta-Hsueh Road, Hsinchu 30010, Taiwan

(Received 4 October 2012; accepted 23 January 2013; published online 5 February 2013)

In this report, we design and utilize one-dimensional photonic crystal ring resonators (1D PhCRRs) to realize InGaAsP/SiO_2 hybrid lasers via adhesive bonding technique. Single-mode lasing with low threshold from the dielectric mode is observed. To further design a nanocavity with mode gap effect in 1D PhCRR results in the reduced lasing threshold and increased vertical laser emissions, owing to the reduced dielectric mode volume and the broken rotational symmetry by the nanocavity. Such hybrid lasers based on 1D PhC rings provides good geometric integration ability and new scenario for designing versatile devices in photonic integrated circuits. © *2013 American Institute of Physics*. [http://dx.doi.org/10.1063/1.4790618]

Two-dimensional photonic crystal ring resonators (2D PhCRRs)[1,2] have been widely applied for constructing versatile photonic integrated circuits (PICs) via proper bus photonic crystal (PhC) waveguides. Comparing with traditional microring resonators, light can operate at slow light region[3] or recycle with low loss via photonic band gap effect in 2D PhCRRs with compact ring sizes, which are beneficial for efficient lasers[4–7] in PICs. In addition to lasers, a variety of functional devices based on 2D PhCRRs, such as add-drop filters,[8,9] logical units,[10,11] optical buffers,[12] and sensors,[13] have also been proposed and demonstrated recently. However, using 2D PhCs leads to large device footprint, and the lattice geometry restricts the integration ability. Although micro-disks (MDs) with different periodic nanostructures[14,15] can overcome these two drawbacks owing to their small device footprints and capabilities for ridge waveguide coupling, the high-order modes in MDs still blemish them for serving as lasers. Another feasible solution is encircling 1D PhC nanobeam (NB), a ridge waveguide with 1D PhCs widely investigated recently for constructing low-loss resonators,[16–19] to form 1D PhCRR as shown in Fig. 1(a). 1D PhCRR has small device footprint and high integration flexibility in PICs via ridge waveguide coupling without PhC lattice geometry restrictions. Recently, 1D PhCRRs have been studied in slow light applications,[20,21] while the other applications are still scarce in the literatures. In this report, we design 1D PhCRRs on SiO_2 to realize InGaAsP/SiO_2 hybrid lasers.[22] Single-mode lasing from the dielectric modes in 1D PhCRRs are observed and identified. And the altered dielectric mode lasing properties when inducing a nanocavity in 1D PhCRR are also investigated.

Scheme of 1D PhCRR (InGaAsP with index $n_{\mathrm{InGaAsP}} \sim 3.4$) is shown in Fig. 1(a), where the underlying substrate provides mechanically stable support for 1D PhCRR that cannot be achieved in a suspended slab. Without inducing significant optical losses, low index ($\sim$1.44) SiO_2 with high thermal conductivity and low cost is a good candidate for the underlying substrate. The parameters of 1D PhCRR, including lattice constant a, air-hole radius r, ring width w, and thickness t, are defined in Figs. 1(a) and 1(b). With $a = 400$ nm, $r/a = 0.27$, $w = 1.3a$, $t = 190$ nm, and total period number P of 28, the simulated dielectric mode profile in electric field in 1D PhCRR by 3D finite-element method (FEM) is shown in Fig. 1(c). This dielectric mode in 1D PhCRR is equivalent to that at the band-edge ($k = \pi/a$ in the band diagram shown in Fig. 1(d)) in 1D PhC NB via 3D plane wave expansion (PWE) method, owing to their matching in $\varepsilon|E|^2$ fields and frequencies shown in Fig. 1(d). The dielectric mode with good field overlapping with the dielectric region (that is, high confinement factor γ_d, defined as the ratio of mode energy in dielectric region) and slow light effect at the band-edge will provide enhanced light-matter interactions for serving as an efficient laser.

To understand the dielectric mode properties in 1D PhCRR, with fixed w and r/a ratio of 1.3a and 0.27, we calculate its Q and γ_d factors as a function of P, as shown in

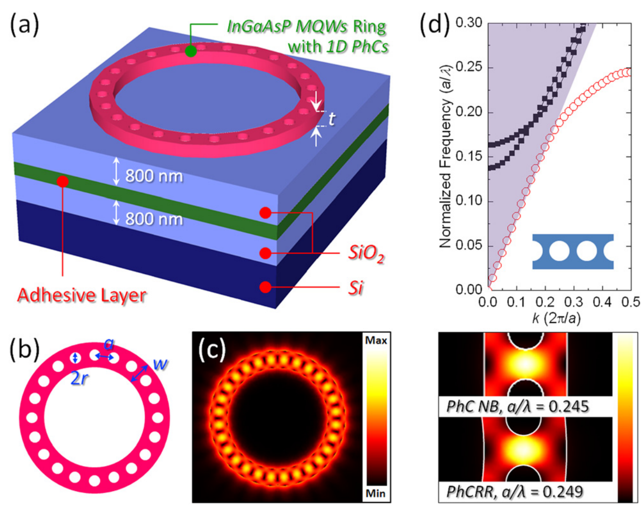

FIG. 1. (a) Scheme of 1D PhCRR on SiO_2 with adhesive layer. (b) Parameters of 1D PhCRR and (c) the simulated dielectric mode profile in electric field by 3D FEM. (d) Band diagram of 1D PhC NB via 3D PWE. The dielectric mode in 1D PhCRR matches well with that at $k_x = \pi/a$ in 1D PhC NB in $\varepsilon|E|^2$ fields and frequencies.

a)Electronic mail: potsung@mail.nctu.edu.tw.

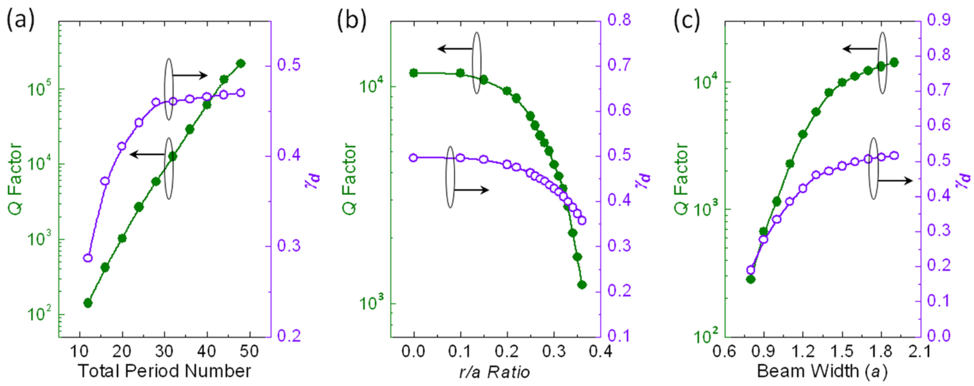

FIG. 2. Theoretic Q and γ_d factors of the dielectric modes in 1D PhCRRs on SiO_2 as (a) a function of P from 12 to 48 under fixed w and r/a ratio of 1.3a and 0.27, (b) a function of r/a ratio under fixed P and w of 28 and 1.3a, and (c) a function of w under fixed P and r/a ratio of 28 and 0.27. The parameters t and a are fixed at 190 and 400 nm in (a)-(c).

Fig. 2(a), which both increase with P owing to the decreased bend loss of the enlarged ring size. Then, with fixed P of 28, the influences of r/a and w on Q and γ_d factors are investigated individually. In Fig. 2(b), with fixed w of 1.3a, both Q and γ_d factors increase when r/a decreases because of the increased effective index. Likewise, in Fig. 2(c), with fixed r/a of 0.27, both Q and γ_d factors increase with w owing to the increased effective index. When $w > 1.1a$, Q and γ_d factors larger than 2000 and 0.4 are sufficient for lasing.

The first step of the fabrication process shown in Fig. 3 to realize 1D PhCRR on SiO_2 is transferring III-V active material, a compressive-strained InGaAsP multi-quantum-wells (MQWs) on InP with InGaAs etching stop layer, denoted as wafer A in Fig. 3, onto SiO_2. The thickness and photoluminescence peak of MQWs are 190 nm and near 1550 nm. MQWs and a silicon (Si) wafer (denoted as wafer B in Fig. 3) are both deposited 800 nm SiO_2 layers by plasma enhanced chemical vapor deposition (PECVD) at 80 °C. Subsequently, we joint these two wafers via DVS-bis-benzocyclobutene (BCB, Cyclotene-4022-35, Dow Chemical Company) adhesive bonding technique,[23,24] as illustrated below in details:

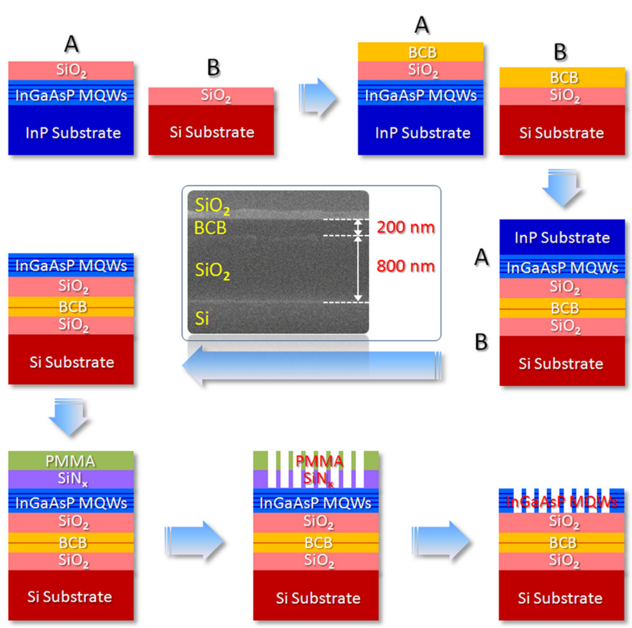

FIG. 3. Flow chart of manufacturing 1D PhCRRs on SiO_2. The inset SEM picture shows the cross-section of the BCB bonding interface.

1. The BCB is spin-coated (6000 rpm for 240 sec) on MQWs and Si wafers with SiO_2.
2. The two wafers are pre-cured at 60 °C for 4 min and then clamped together under uniform pressure of 130 kPa at 250 °C for 2 h.

With diluted BCB (mesitylene: BCB = 1:3), after step 2, the thickness of BCB adhesive layer is as thin as 200 nm, shown as the inset cross-sectional scanning electron microscope (SEM) picture in Fig. 3. The InP substrate of MQWs, InGaAs etching-stop, and InP capping layers are removed via diluted HCl, solution of $H_3PO_4/H_2O_2/H_2O = 1:1:8$, and diluted HCl wet etching at room temperature in sequence to leave MQWs on SiO_2. Then the MQWs on SiO_2 are followed by a series of nanofabrication process illustrated below to manufacture PhC nanostructures.

1. Deposit 70 nm SiN_x hard mask on MQWs by PECVD.
2. Spin-coat 240 nm electron-beam (e-beam) resist (polymethylmethacrylate, PMMA) on SiN_x hard mask.
3. Define PhC patterns on PMMA via e-beam lithography.
4. Transfer PhC patterns from PMMA to SiN_x hard mask and MQWs in sequence via reactive ion etching and inductively coupled plasma dry etching at room temperature.

Top- and tilted-view SEM pictures of 1D PhCRR on SiO_2 are shown in Figs. 4(a) and 4(b), where the parameters t, a, r/a, P, and w are 190 nm, 400 nm, 0.27, 28, and 1.3a, respectively. Theoretic mode volume V_{eff}, Q, and γ_d factors of the dielectric mode are 2.9 $(\lambda/n_{InGaAsP})$,[3] 5800, and 0.460. In Fig. 4(b), the underlying SiO_2 can be clearly observed. The patterns surrounding the 1D PhCRR are designed to reduce the proximity effect during e-beam lithography, which will not significantly affect the dielectric modal properties in 1D PhCRR. This is confirmed via the almost

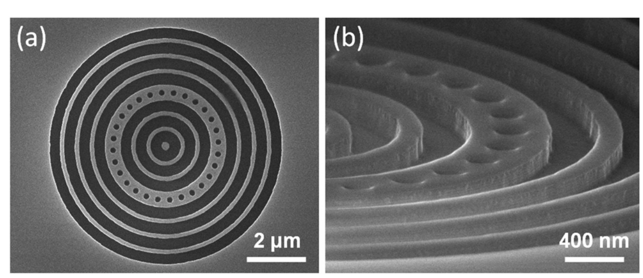

FIG. 4. (a) Top- and (b) tilted-view SEM pictures of 1D PhCRR with $P = 28$.

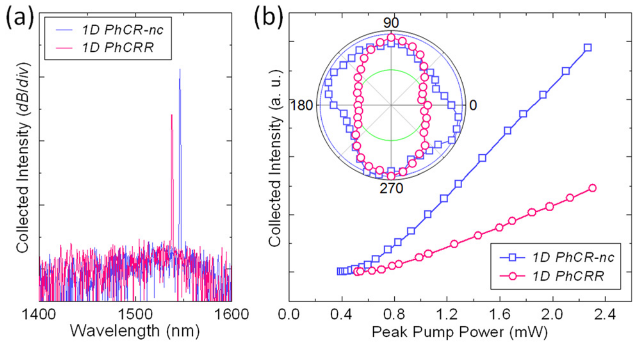

FIG. 5. (a) Single-mode lasing spectra, (b) L-L curves, and polarizations of the dielectric modes in 1D PhCRR and PhCR-nc with the same r/a (0.27), a (400 nm), and w (520 nm).

invariant theoretic wavelengths (0.3 nm difference), Qs (7% difference), and dielectric modes profiles in 1D PhCRRs with and without the surrounding patterns via 3D FEM.

We then characterize 1D PhCRR shown in Fig. 4 via diode laser pulse with wavelength of 845 nm, 2% duty cycle, and spot size of 6 μm in diameter. Single-mode lasing spectrum at wavelength near 1538 nm with side-mode suppression-ratio (SMSR) of 25 dB are obtained and shown in Fig. 5(a). Unlike the MDs with periodic nanostructures,[14,15] only one mode has sufficient Q for lasing in 1D PhCRR. A lasing threshold of 0.57 mW (effective threshold $\sim$36 μW) is estimated from the light-in light-out (L-L) curve shown in Fig. 5(b). Moreover, dissimilar to highly linear-polarized laser emissions of the dielectric modes in 1D PhC NB,[18,19] the emissions from 1D PhCRR exhibit a low polarized degree (PD) of 2.3, shown in the inset of Fig. 5(b). Owing to the rotational symmetry of the ring, E_x and E_y fields of the dielectric mode in 1D PhCRR are identical, which means the laser emission is dominated by neither E_x nor E_y fields and should be un-polarized ideally. PD > 1 in experiments is attributed to the fabrication imperfections of the characterized device. In addition, we also demonstrate 1D PhCRRs with different P. Single-mode lasing from the dielectric mode can be still observed when $P = 24$ only, whose device footprint is as tiny as 21 μm^2.

Comparing with the traditional microring resonators, in addition to the slow light effect mentioned before, the other significant benefit of 1D PhCRR is that the mode properties can be altered via purposely tuned PhCs. To show this feature, we linearly shrink the air-hole radii of 1D PhCRR under fixed a of 400 nm from the top (r) to the side region (r'), as shown in Fig. 6(a). This forms a 1D PhCR nanocavity (1D PhCR-nc) with mode gap effect, where $\Delta r/a$ is defined as $r/a - r'/a$. In Fig. 6(b), with $\Delta r/a$ of 0.02 and the same parameters as for 1D PhCRR, the dielectric mode in 1D PhCR-nc shows significant field enhancement in the cavity region than that in PhCRR, which leads to a reduced V_{eff} of 1.7 $(\lambda/n_{InGaAsP})^3$ while there are no significant reductions in Q ($\sim$5700) and γ_d ($\sim$0.456) factors.

In measurements, single-mode lasing with SMSR over 30 dB is observed from 1D PhCR-nc on SiO_2 with $\Delta r/a$ of 0.02 and the same parameters as for 1D PhCRR, as shown in Fig. 5(a). The lasing wavelength of 1D PhCR-nc near

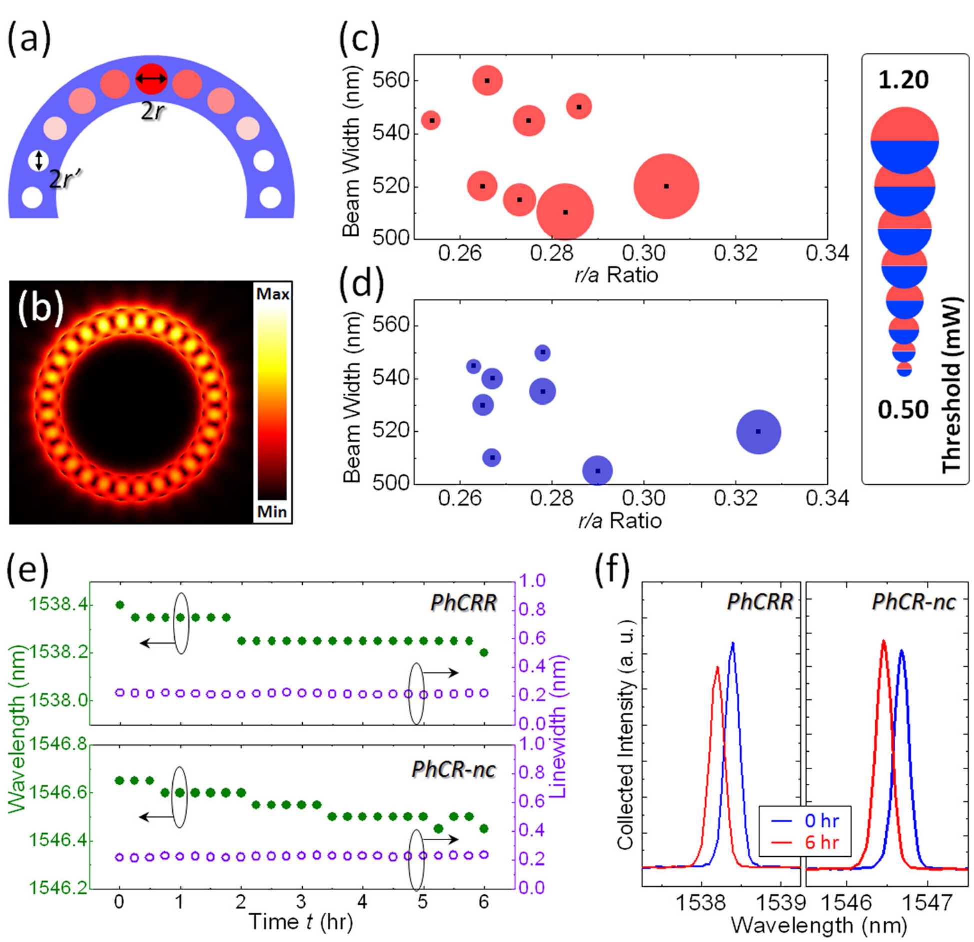

FIG. 6. (a) Design of 1D PhCR-nc and (b) its theoretic dielectric mode profile in electric field via 3D FEM. Lasing thresholds of the dielectric modes in 1D (c) PhCRRs and (d) PhCR-ncs under different w and r/a. (e) Lasing wavelengths and line-widths of 1D PhCRR and PhCR-nc as functions of t. (f) Lasing spectra of 1D PhCRR and PhCR-nc when $t = 0$ and 6 h.

1546 nm shows a red shift of 8.0 nm than that of 1D PhCRR, which agrees well with the theoretic value of 11.4 nm via 3D FEM. More noteworthy is that the L-L curve of 1D PhCR-nc in Fig. 5(b) shows a lower threshold of 0.46 mW (effective threshold $\sim$29 μW) and larger slope efficiency than those of 1D PhCRR. With almost the same Q and γ_d factors of the dielectric modes in 1D PhCRR and PhCR-nc, smaller V_{eff} in 1D PhCR-nc means larger *Purcell* factor, that is, stronger coupling between spontaneous emission and lasing mode,[25] which leads to lower threshold of 1D PhCR-nc than that of PhCRR. In addition, the existence of nanocavity leads to the rotational symmetry breaking and changes the far-field profile of the dielectric mode, thus resulting in more vertical emissions[15,26] and larger slope efficiency of 1D PhCR-nc than those in 1D PhCRR. Moreover, the laser emissions from 1D PhCR-nc also exhibit a low PD of 1.5, shown in the inset of Fig. 5(b). This is because neither E_x nor E_y fields significantly dominate the dielectric mode in 1D PhCR-nc. Furthermore, the thresholds of 1D PhCRRs and PhCR-ncs with different w and r/a are shown in Figs. 6(c) and 6(d). The thresholds of 1D PhCRRs are always higher than those of 1D PhCR-ncs, owing to their differences in V_{eff} of the dielectric modes as mentioned before. The thresholds of 1D PhCRRs and PhCR-ncs both decrease with decreasing r/a and increase with decreasing w, which strongly correlate with the variations of γ_d factors under different r/a and w shown in Figs. 2(b) and 2(c).

To know the long term stability of 1D PhCRR and PhCR-nc, the devices are excited continuously for 6 h by fixed pump power of 1.5 mW. Lasing wavelengths and linewidths of 1D PhCRR and PhCR-nc as functions of excitation time t are shown in Fig. 6(e). After 6 h, both of them show slight blue shifts of 0.2 nm in lasing wavelength owing to the surface oxidation of InGaAsP and almost invariant linewidths. The lasing spectra of 1D PhCRR and PhCR-nc at $t=0$ and 6 h are shown in Fig. 6(f). These results not only show the long term stabilities of lasing from 1D PhCRR and PhCR-nc but also confirm the thermal stability of the BCB adhesive layer under present pump condition.

In summary, we have proposed and investigated the dielectric mode properties in 1D PhCRR on SiO_2. Via BCB adhesive bonding technique and a series of nanofabrication process, the designed 1D PhCRR is utilized to demonstrate InGaAsP/SiO_2 hybrid lasers with low effective threshold ($\sim$36 μW) and small device footprint. To further design a nanocavity with mode gap effect in 1D PhCRR to form a 1D PhC-nc will result in the reduced lasing threshold ($\sim$29 μW) and increased vertical laser emissions owing to the reduced dielectric mode volume and the rotational symmetry breaking by the nanocavity. In addition, the long term stabilities of lasing from 1D PhCRR and PhCR-nc are also confirmed. We believe this kind of resonators based on 1D PhCR with small device footprints and good integration ability without lattice geometry restriction can provide new scenarios as efficient active light sources and other functional passive devices in versatile PICs.

This work is supported by Taiwan's National Science Council (NSC) under Contracts Nos. NSC-100-2221-E-009-109-MY3, NSC-101-2221-E-009-054-MY2, and NSC-101-3113-P-009-004. The authors would like to thank the helps from Professor Jin-Wei Shi in Department of Electrical Engineering, National Central University (NCU), Taiwan, and Center for Nano Science and Technology (CNST) of National Chiao Tung University (NCTU), Taiwan.

[1]W. Y. Chiu, T. W. Huang, Y. H. Wu, Y. J. Chan, C. H. Hou, H. T. Chien, and C. C. Chen, Opt. Express **15**, 15500 (2007).
[2]S. H. Jeong, N. Yamamoto, J. Sugisaka, M. Okano, and K. Komori, J. Opt. Soc. Am. B **24**, 1951 (2007).
[3]T. F. Krauss, J. Phys. D **40**, 2666 (2007).
[4]S. H. Kim, H. Y. Ryu, H. G. Park, G. H. Kim, Y. S. Choi, Y. H. Lee, and J. S. Kim, Appl. Phys. Lett. **81**, 2499 (2002).
[5]A. R. Alija, L. J. Martínez, P. A. Postigo, C. Seassal, and P. Viktorovitch, Appl. Phys. Lett. **89**, 101102 (2006).
[6]P. A. Postigo, A. R. Alija, L. J. Martínez, M. L. Dotor, D. Golmayo, J. Sánchez-Dehesa, C. Seassal, P. Viktorovitch, M. Galli, A. Politi, M. Patrini, and L. C. Andreani, Photonics Nanostruct. **5**, 79 (2007).
[7]K. Kitamura, M. Nishimoto, K. Sakai, and S. Noda, in CLEO Science and Innovations Conference, San Jose, CCA, 8 May 2012, paper CTu1N.3.
[8]Z. Qiang, W. Zhou, and R. A. Soref, Opt. Express **15**, 1823 (2007).
[9]X. Chen, Z. Qiang, D. Zhao, H. Li, Y. Qiu, W. Yang, and W. Zhou, Opt. Express **17**, 19808 (2009).
[10]P. Andalib and N. Granpayeh, J. Opt. Soc. Am. B **26**, 10 (2009).
[11]J. Bai, J. Wang, J. Jiang, X. Chen, H. Li, Y. Qiu, and Z. Qiang, Appl. Opt. **48**, 6923 (2009).
[12]J. Sugisaka, N. Yamamoto, M. Okano, K. Komori, and M. Itoh, J. Opt. Soc. Am. B **29**, 1521 (2012).
[13]F. Hsiao and C. Lee, IEEE Sens. J. **10**, 1185 (2010).
[14]K. Nozaki, A. Nakagawa, D. Sano, and T. Baba, IEEE J. Sel. Top. Quantum Electron. **9**, 1355 (2003).
[15]Y. Zhang, C. Hamsen, J. T. Choy, Y. Huang, J. H. Ryou, R. D. Dupuis, and M. Lončar, Opt. Lett. **36**, 2704 (2011).
[16]M. Notomi, E. Kuramochi, and H. Taniyama, Opt. Express **16**, 11095 (2008).
[17]P. B. Deotare, M. W. McCutcheon, I. W. Frank, M. Khan, and M. Lončar, Appl. Phys. Lett. **94**, 121106 (2009).
[18]Y. Zhang, M. Khan, Y. Huang, J. H. Ryou, P. B. Deotare, R. Dupuis, and M. Lončar, Appl. Phys. Lett. **97**, 051104 (2010).
[19]B. H. Ahn, J. H. Kang, M. K. Kim, J. H. Song, B. Min, K. S. Kim, and Y. H. Lee, Opt. Express **18**, 5654 (2010).
[20]D. Goldring, U. Levy, and D. Mendlovic, Opt. Express **15**, 3156 (2007).
[21]J. Y. Lee and P. M. Fauchet, Opt. Lett. **37**, 58 (2012).
[22]A. W. Fang, H. Park, Y. Kuo, R. Jones, O. Cohen, D. Liang, O. Raday, M. N. Sysak, M. J. Paniccia, and J. E. Bowers, Mater. Today **10**, 28 (2007).
[23]G. Roelkens, J. Van Campenhout, J. Brouckaert, D. Van Thourhout, R. Baets, P. R. Romeo, P. Regreny, A. Kazmierczak, C. Seassal, X. Letartre, G. Hollinger, J. M. Fedeli, L. Di Cioccio, and C. Lagahe-Blanchard, Mater. Today **10**, 36 (2007).
[24]M. Yokoyama, T. Yasuda, H. Takagi, H. Yamada, N. Fukuhara, M. Hata, M. Sugiyama, Y. Nakano, M. Takenaka, and S. Takagi, Appl. Phys. Express **2**, 124501 (2009).
[25]K. Nozaki, S. Kita, and T. Baba, Opt. Express **15**, 7506 (2007).
[26]L. Mahler, A. Tredicucci, F. Beltram, C. Walther, J. Faist, B. Witzigmann, H. E. Beere, and D. A. Ritchie, Nat. Photonics **3**, 46 (2009).